1082 *Organometallics* **2005,** *24,* 1082−1090

Pincer "Hemilabile" Effect. PCN Platinum(II) Complexes with Different Amine "Arm Length"

Elena Poverenov,[†] Mark Gandelman,[†] Linda J. W. Shimon,[‡] Haim Rozenberg,[‡]
Yehoshoa Ben-David,[†] and David Milstein*[,†]

Department of Organic Chemistry and Unit of Chemical Research Support,
The Weizmann Institute of Science, Rehovot, 76100, Israel

Received October 21, 2004

The reactivity of the "long arm" PCN-type pincer ligand $C_6H_4[CH_2P(tBu)_2](CH_2)_2N(CH_3)_2$ (**1**), which forms complexes bearing a six-membered amine chelate and a five-membered phosphine chelate, was compared with that of the new "normal" PCN ligand $C_6H_4[CH_2P(tBu)_2](CH_2)N(CH_2CH_3)_2$ (**2**), which leads to formation of complexes bearing two five-membered chelates. The chloride complexes (PCN)PtCl (**3**, **4**) and the unsaturated cationic complexes $[(PCN)Pt]^+X^-$ (X = BF_4, OTf) (**5**, **6**, **7**), based on both PCN ligands, were prepared and reacted with different reagents to give aqua, $[(PCN\text{-}\mathbf{1})Pt(H_2O)]^+BF_4^-$ (**10**); hydroxo, (PCN-**1**)Pt(OH) (**11**); carbonyl $[(PCN)Pt(CO)]^+BF_4^-$ (**8**, **9**); and hydride, (PCN-**1**)PtH (**16**) complexes. The structures of complexes **4**, **6**, **8**, **10**, **11**, and **12** were determined by X-ray crystallography. When both carbonyl complexes were treated with hydrogen gas, the "long arm" PCN-**1**-based complex **8** led to formation of a trimeric cluster, $[C_6H_6[CH_2P(tBu)_2](CH_2)_2N(CH_3)_2Pt(CO)]_3$ (**12**), while the "normal" PCN-based complex **9** remained unchanged under the same conditions. This observation clearly demonstrates the very significant effect of the amine arm length (five- vs six-membered chelate) on the hemilability of the ligand and the reactivity of the corresponding complexes.

Introduction

Late transition metal pincer-type complexes containing a T-shaped X−C−X (X = N, P) ligand core play an important role in organometallic chemistry. Such tridentate ligands enhance the stability of the complexes and allow the manipulation of steric and electronic parameters, which control reactivity at the metal center.[1]

In NCN (**A$_1$**) ligand-based complexes, which were extensively studied by van Koten and co-workers, the hard, σ-donating amine groups are not always spectator ligands and can participate in metal-centered reactions, providing the corresponding NCN complexes with interesting stoichiometric and catalytic properties.[1a,2] PCP-ligand-based complexes (**A$_2$**) exhibit high chelate stability and were utilized in the activation of strong bonds, stabilization of unstable elusive compounds, and various catalytic transformations.[1]

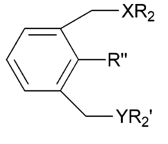

R, R' = alkyl,aryl. R'' = H,CH$_3$, OCH$_3$, OH.
A$_1$: X=Y=N (NCN), **A$_2$**: X=Y=P (PCP), X=P; **A$_3$**:Y=N (PCN).

Recently, the mixed PCN ligand (**A$_3$**) was synthesized in our group, and it was shown that such a ligand could benefit from advantages of both the NCN and PCP ligand systems. PCN-based rhodium complexes were utilized in selective C−C and C−H bond activation,[3] in catalytic C−N bond activation,[4] and in novel catalytic azine reactivity.[5] Carbene- and diazo-PCN-Rh(I) complexes were reported[6] and utilized in mechanistic studies of carbene formation from diazo compounds.[6b] Using PCN-based complexes, medium effects on highly unsaturated Rh(III) complexes were investigated and a dearomatized methylene arenium system was obtained when stabilizing solvents and/or counteranions were absent.[7] Moreover, a PCN-based system allowed for the first time the observation of a single-step metal insertion into a C−C bond and the evaluation of the kinetic parameters of this process.[8] Hemilabile PCO complexes were also reported to be involved in C−C activation.[9]

It is expected that the amine "arm" will be involved in more labile coordination to late transition metals in

---

* Corresponding author. Fax: 972-8-9344142. E-mail: david.milstein@weizmann.ac.il.

[†] Department of Organic Chemistry.

[‡] Unit of Chemical Research Support.

(1) Recent reviews: (a) Albrecht, M.; van Koten, G. *Angew. Chem., Int. Ed.* **2001**, *40*, 3750. (b) van der Boom, M. E.; Milstein, D. *Chem. Rev.* **2003**, *103*, 1759. (c) (g) Jensen, C. J. *Chem. Commun.* **1999**, 2443. (d) Singleton, J. T. *Tetrahedron* **2003**, *59*, 1837. (e) Vigalok, A.; Milstein, D. *Acc. Chem. Res.* **2001**, *34*, 798. (f) Rybtchinski, B.; Milstein, D. *Angew. Chem., Int. Ed. Engl.* **1999**, *38*, 870. (g) Milstein, D. *Pure Appl. Chem.* **2003**, *75*, 2003. (h) Milstein, D.; Rybtchinski, B. *ACS Symp. Ser.* **2004**, *885*, 70.

(2) (a) van Koten, G. *Pure Appl. Chem.* **1989**, *62*, 1681. (c) Grove, D. M.; van Koten, G.; Verschuuren, A. H. M. *J. Mol. Catal.* **1988**, *45*, 169. (d) van Beek, J. A. M.; van Koten, G.; Smeets, W. J. J.; Spek, A. L. *J. Am. Chem. Soc.* **1986**, *108*, 5010.

(3) (a) Gandelman, M.; Vigalok, A.; Shimon, L. J. W.; Milstein, D. *Organometallics*, **1997**, *16*, 3981. (b) Gandelman, M.; Shimon, L.; Milstein, D. *Chem. Eur. J.* **2003**, *9*, 4295.

(4) Gandelman, M.; Milstein, D. *Chem. Commun.* **2000**, 1603.

(5) Rybtchinski, B.; Cohen, R.; Gandelman, M.; Shimon. L. J. W.; Martin, J. M. L.; Milstein, D. *Angew. Chem., Int. Ed.* **2003**, *115*, 1993.

(6) (a) Gandelman, M.; Rybtchinski, B.; Ashkenazi, N.; Gauvin, R.; Milstein, D. *J. Am. Chem. Soc.* **2001**, *123*, 5372. (b) Cohen, R.; Rybtchinski, B.; Gandelman, M.; Rozenberg, M.; Martin, J. M. L.; Milstein, D. *J. Am. Chem. Soc.* **2003**, *125*, 6532.

(7) Gandelman, M.; Konstantinovski, L.; Rozenberg, H.; Milstein, D. *Chem. Eur. J.* **2003**, *9*, 2595.

10.1021/om049182m CCC: $30.25

Scheme 1

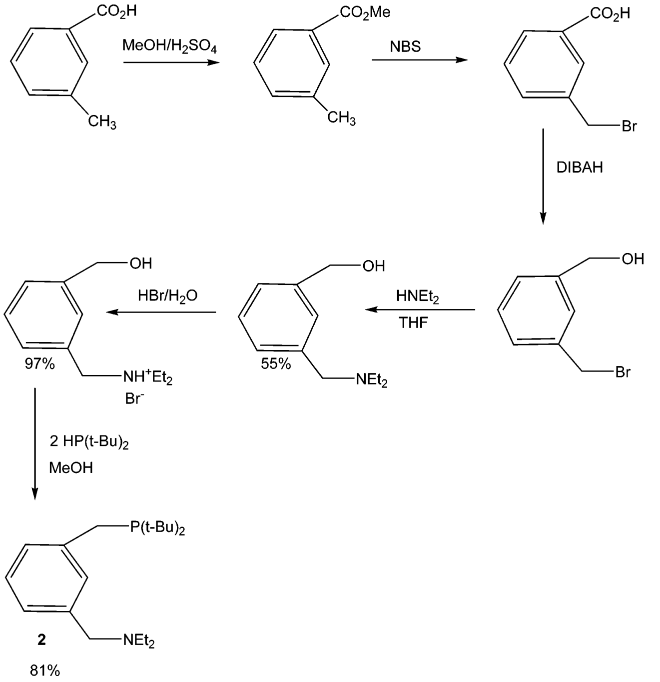

comparison with a phosphine,[10] particularly when low oxidation states are involved. Such on/off coordination could provide the system with additional reactivity patterns, and it was of interest to explore the influence of the amine “arm” length on the hemilability of the system.

Recently we reported on the synthesis of the “long arm” PCN ligand **1** bearing a dimethylene unit as a connector of the aromatic ring and the amine group.[11] This ligand enabled the generation and stabilization of rare anionic dialkyl, diaryl, and dihydride Pt complexes (which bear no stabilizing π-acceptors) due to the labile coordination of the amine arm. Here we present our studies on the chemical properties and reactivity of Pt complexes based on the PCN ligand **1**. To understand the role of the additional methylene group in the amine “arm” of ligand **1**, the new PCN ligand **2**, which bears a shorter arm, was synthesized and the chemical behavior of **1** and **2** was compared.

Results and Discussion

Synthesis of the PCN Ligand 2. The new PCN ligand **2** was synthesized from 3-(bromomethyl)benzyl alcohol, which was obtained by esterification, bromination, and reduction of 3-(methyl)benzoic acid according to a literature procedure.[12] The resulting 3-(bromomethyl)benzyl alcohol was reacted with a slight excess of diethylamine at room temperature to give 3-(diethylaminomethyl)benzyl alcohol, which was brominated with an aqueous solution of HBr to yield 3-(diethylaminomethyl)benzyl bromide·HBr salt. Reaction of the latter with di-*tert*-butylphosphine at 50 °C for 48 h yielded the clean ligand **2** (Scheme 1).

Scheme 2

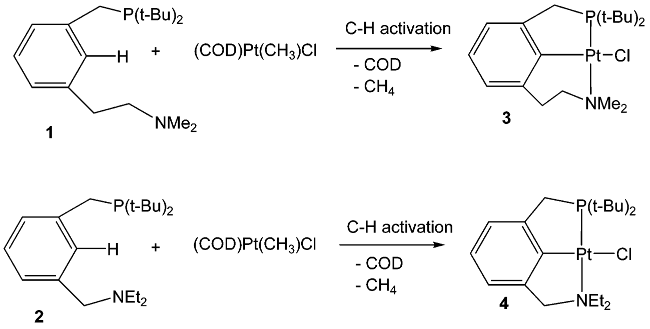

Table 1. Selected Bond Lengths and Angles of Complex 4

bond length	Å	angle	deg
Pt(1)−C(1)	1.971(5)	C(1)−Pt(1)−N(1)	82.84(19)
Pt(1)−N(1)	2.192(4)	C(1)−Pt(1)−P(2)	83.58(15)
Pt(1)−P(2)	2.217(13)	C(1)−Pt(1)−Cl(3)	174.36(14)
Pt(1)−Cl(3)	2.408(13)	N(1)−Pt(1)−P(2)	166.25(12)
N(1)−C(14)	1.500(7)	N(1)−Pt(1)−Cl(3)	93.22(12)
N(1)−C(12)	1.500(7)	P(2)−Pt(1)−Cl(3)	100.48(5)
P(2)−C(21)	1.849(5)	C(14)−N(1)−C(12)	108.3(4)
P(2)−C(23)	1.870(5)	C(14)−N(1)−Pt(1)	109.9(3)

Synthesis and Characterization of PCN-Based Platinum Chloride Complexes. “Long arm” and “normal arm” PCN-based platinum chloride complexes were obtained as a result of C−H activation and methane elimination reactions (Scheme 2). We have recently reported the synthesis of complex **3**.[11] Complex **4** was quantitatively prepared by addition of a THF solution of ligand **2** to (COD)Pt(CH_3)Cl (COD = cyclooctadiene), followed by heating at 100 °C for 30 min. The $^{31}P\{^1H\}$ NMR spectrum of **4** exhibits a singlet at 64.31 ppm with Pt satellites (J_{Pt-P} = 4294 Hz), and in the $^{13}C\{^1H\}$ NMR spectrum the ipso carbon shows a doublet at 149.22 ppm (J_{P-C} = 29 Hz). Colorless plates of complex **4** suitable for a single-crystal X-ray analysis were obtained by crystallization of **4** from a benzene/pentane solution at room temperature (Figure 1). Selected bond lengths and bond angles are given in Table 1.

Like in the case of complex **3**,[11] complex **4** has a square-planar structure. The main difference between the two structures is the P−Pt−N angle, which is almost linear (175.2°) in the case of complex **3**, while in complex **4** this angle is 166.2°. These values reflect the lower

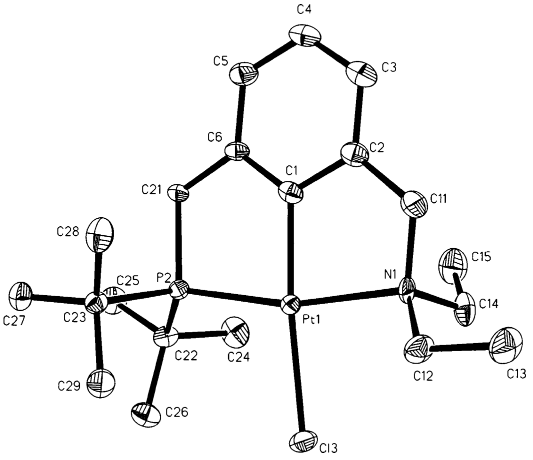

Figure 1. ORTEP view of a molecule of complex **4**. Hydrogen atoms are omitted for clarity.

---

(8) Gandelman, M.; Vigalok, A.; Kontantinovski, L.; Milstein, D. *J. Am. Chem. Soc.* **2000**, *122*, 9848.

(9) Rybtchinski, B.; Oevers, S.; Montag, M.; Vigalok, A.; Rogenberg, H.; Martin, J. M. L.; Milstein, D. *J. Am. Chem. Soc.* **2001**, *123*, 9064.

(10) Crabtree, R. H. *The Organometallic Chemistry of The Transition Metals*; John Wiley & Sons: New York, 1994.

(11) Poverenov, E.; Gandelman, M.; Shimon, L. J. W.; Rozenberg, H.; Ben-David, Y.; Milstein, D. *Chem. Eur. J.* **2004**, *10*, 4673.

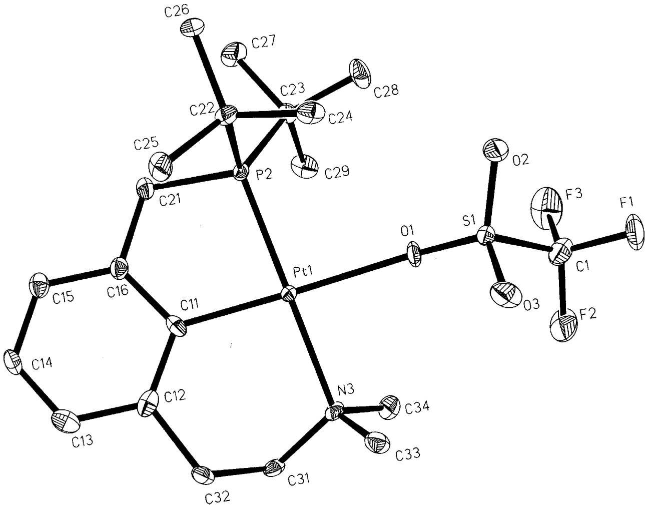

Figure 2. ORTEP view of a molecule of complex **6**. Hydrogen atoms are omitted for clarity.

Scheme 3

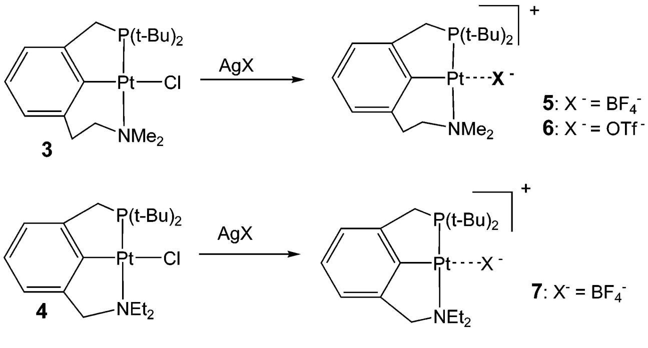

rigidity of the six-membered ring in comparison with the five-membered one, providing complex **3** with considerable flexibility.

Synthesis and Reactions of Cationic Complexes. The electron-rich and bulky PCN ligands **1** and **2** can readily stabilize cationic Pt(II) complexes. When AgX ($X = BF_4^-$, $CF_3SO_3^-$) was added to a CH_2Cl_2 solution or (in case of $CF_3SO_3^-$) THF solution of **3**, the cationic complexes **5** and **6** were obtained after 1 h of stirring at room temperature (Scheme 3). The $^{31}P\{^1H\}$ NMR spectrum of **5** exhibits a singlet at 69.60 ppm with Pt satellites ($J_{Pt-P} = 3985$ Hz), and in the $^{13}C\{^1H\}$ NMR spectrum the ipso carbon exhibits a doublet at 150.71 ppm ($J_{P-C} = 10$ Hz). In the ^{19}F NMR spectrum, the BF_4^- anion gives rise to a broad singlet at −162.27 ppm. Since this value is significantly different from the chemical shift of noncoordinated BF_4^- (−151.23 ppm, narrow peak, in CD_2Cl_2), and based on previously reported coordinated and noncoordinated BF_4^- unsaturated complexes,[7] it is clear that in this case BF_4^- is coordinated to the metal.

Complex **6** was also characterized by multinuclear NMR techniques. In the $^{31}P\{^1H\}$ NMR spectrum it gives rise to a singlet at 66.52 ppm with Pt satellites ($J_{Pt-P} = 4005$ Hz). In the ^{19}F NMR spectrum the coordinated OTf group was observed as a singlet at −77.61 ppm.

Crystallization of **6** from a THF/pentane mixture resulted in colorless needles, which were suitable for X-ray single-crystal analysis (Figure 2). The platinum atom is located in the center of a slightly distorted square-planar structure, with the triflate anion being coordinated to platinum *trans* to the aromatic ring. Selected bond lengths and bond angles of **6** are given in Table 2.

Scheme 4

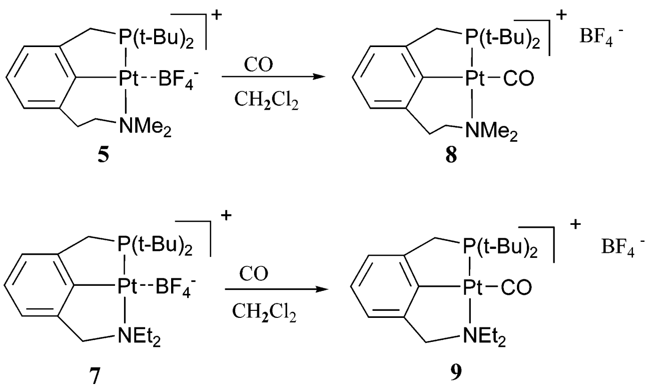

Table 2. Selected Bond Lengths and Angles of Complex 6

bond length	Å	angle	deg
Pt(1)−C(11)	2.005(7)	C(11)−Pt(1)−N(3)	95.1(3)
Pt(1)−N(3)	2.168(6)	C(11)−Pt(1)−P(2)	84.6(2)
Pt(1)−P(2)	2.248(17)	N(3)−Pt(1)−P(2)	174.4(17)
Pt(1)−O(1)	2.249(5)	C(11)−Pt(1)−O(1)	178.2(3)
S(1)−O(1)	1.468(5)	P(2)−Pt(1)−O(1)	94.0(14)
N(3)−C(33)	1.472(9)	O(2)−S(1)−O(3)	116.1(4)
P(2)−C(21)	1.832(7)	C(12)−C(11)−Pt(1)	124.7(6)
C(1)−F(1)	1.345(10)	S(1)−O(1)−Pt(1)	144.5(4)

Complex **4**, based on the "normal arm" PCN ligand, also undergoes facile abstraction of the chloride ligand by silver salts. Reaction of **4** with $AgBF_4$ gave, after 1 h of stirring at room temperature, the cationic complex **7** (Scheme 3). **7** exhibits a single resonance at 63.91 ppm ($J_{Pt-P} = 4195$ Hz) in the $^{31}P\{^1H\}$ NMR spectrum (in C_6D_6), and its ipso carbon appears at 148.41 ppm in the $^{13}C\{^1H\}$ NMR spectrum. The BF_4 counteranion appears in the ^{19}F NMR spectrum (in CD_2Cl_2) at −162.14 ppm, indicating that it is coordinated to the metal center (see above).

Reaction with CO. The weakly coordinated BF_4^- counteranion is easily displaced by better coordinating ligands. When a slight excess of CO was added to a methylene chloride solution of complex **5**, the new carbonyl complex **8** was immediately formed (Scheme 4). The $^{31}P\{^1H\}$ NMR spectrum of **8** shows a singlet at 81.04 ppm with Pt satellites ($J_{Pt-P} = 3045$ Hz). In the $^{13}C\{^1H\}$ NMR spectrum the ipso carbon exhibits a doublet at 150.65 ppm ($J_{P-C} = 9$ Hz), and a peak due to the carbonyl ligand appears at 181.14 ppm as a doublet ($J_{P-C} = 8$ Hz) with Pt satellites ($J_{Pt-C} = 981$ Hz). In the IR spectrum, the carbonyl stretch was observed at 2082 cm^{-1}, indicating little back-bonding, and a relatively low electron density at the metal center. In complex **8** the noncoordinated BF_4 anion appears in the ^{19}F NMR spectrum as a singlet at −153.01 ppm.

Complex **8** was crystallized by slow evaporation of a CH_2Cl_2 solution to give pale yellow prisms, which were appropriate for a single-crystal X-ray analysis. It exhibits a square-planar structure, the carbonyl ligand being coordinated *trans* to the aromatic ring (Figure 3). The counteranion BF_4^- is located out of the coordination sphere. Selected bond lengths and bond angles of complex **8** are given in Table 3. In a similar mode, reaction of complex **7** ("normal arm" PCN-based cationic

---

(12) O'Hanlon, P. J.; Rogers, N. H. Eur. Pat. Appl. AN 406065, 1982.

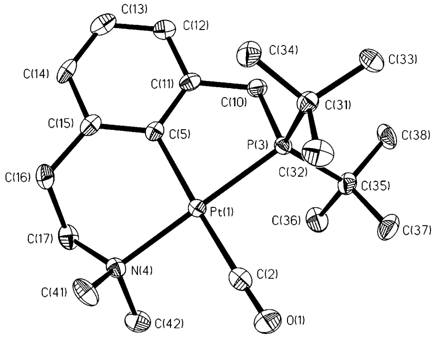

Figure 3. ORTEP view of a molecule of complex **8**.

Table 3. Selected Bond Lengths and Angles of Complex 8

bond length	Å	angle	deg
Pt(1)−C(2)	1.923(4)	C(2)−Pt(1)−C(5)	172.3(18)
Pt(1)−C(5)	2.063(4)	C(2)−Pt(1)−N(4)	88.9(15)
Pt(1)−N(4)	2.158(3)	C(5)−Pt(1)−N(4)	94.4(13)
Pt(1)−P(3)	2.272(11)	C(2)−Pt(1)−P(3)	94.4(12)
O(1)−C(2)	1.143(5)	C(5)−Pt(1)−P(3)	83.1(11)
N(4)−C(17)	1.494(5)	N(4)−Pt(1)−P(3)	172.9(9)
P(3)−C(35)	1.872(4)	O(1)−C(2)−Pt(1)	175.2(5)
C(5)−C(15)	1.411(5)	C(10)−P(3)−Pt(1)	102.9(1)

complex) with CO resulted in the expected carbonyl complex **9** (Scheme 4). This complex exhibits a signal at 80.16 ppm ($J_{\text{Pt-P}}$ = 3264 Hz) in the ^{31}P{^{1}H} NMR spectrum, and the coordinated carbonyl ligand appears at 185.19 ppm (d, $J_{\text{P-C}}$ = 6 Hz) in the ^{13}C{^{1}H} NMR spectrum and gives rise to an absorption at 2085 cm^{-1} in the IR spectrum.

Coordination of Water. Protonation and Deprotonation Reactions. Chemistry of aqua and hydroxo complexes is of significant current interest. With late metal complexes, the water ligand is expected to bind to the metal fairly weakly, and the hydroxo ligand is expected to undergo heterolysis readily.[13] Such complexes may be relevant to catalytic hydration of olefins to form alcohols, under neutral conditions, which is an attractive industrial goal.[14] Aqua complexes of Pt(II) are well known.[15] Stable monomeric Pt(II) hydroxides are less common, because of their high reactivity and tendency to dimerize, and very few of them have been structurally characterized.[16]

Utilizing the PCN ligands, we prepared monomeric aqua and hydroxo Pt complexes. Thus, when a slight excess of H_2O was added to a dichloromethane solution of **5**, quantitative coordination of water was observed to give complex **10** (Scheme 5). The ^{31}P{^{1}H} NMR spectrum of **10** exhibits a single resonance at 67.52 ppm with Pt−P satellites ($J_{\text{Pt-P}}$ = 3950 Hz), and the protons of the coordinated water molecule appear in the ^{1}H NMR spectrum as a broad singlet at 5.12 ppm. Recrystallization of **10** from a THF/pentane solution resulted in colorless prismatic crystals, which were subjected to a single-crystal X-ray analysis (Figure 4). Complex **10** exhibits a square-planar structure with a practically symmetrical arrangement of the four ligands around the Pt center and an outer-sphere BF_4^- counteranion. The metal−oxygen (2.18 Å) and H−O (0.86 Å) bond lengths are similar to those observed in other known late transition metal aqua complexes. According to the X-ray data, there are hydrogen-bonding interactions between protons of the coordinated water molecule and the fluorine atoms of the BF_4 counteranion, the shortest distance being observed between the H(2A) and F^{1} atoms (2.04 Å). These data are in good agreement with other known organometallic complexes that exhibit

Scheme 5

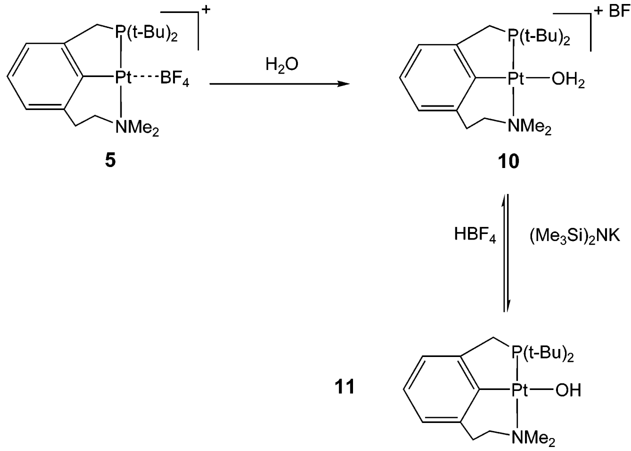

Table 4. Selected Bond Lengths and Angles of Complex 10

bond length	Å	angle	deg
Pt(1)−C(1)	1.99(4)	C(11)−Pt(1)−N(1)	95.9(14)
Pt(1)−N(1)	2.16(3)	C(1)−Pt(1)−O(1)	172.6(14)
Pt(1)−O(1)	2.18(3)	N(1)−Pt(1)−O(1)	88.0(14)
Pt(1)−P(2)	2.23(10)	C(1)−Pt(1)−P(2)	84.0(11)
O(1)−H(1A)	0.86(6)	N(1)−Pt(1)−P(2)	174.0(8)
O(1)−H(2A)	0.86(8)	O(1)−Pt(1)−P(2)	92.7(9)
N(1)−C(11)	1.48(5)	Pt(1)−O(1)−H(1A)	130(3)
H(2A)−F(1)	2.04	O(1)−H(2A)−F(1)	165
P(2)−C(21)	1.82(3)	Pt(1)−O(1)−H(2A)	113(5)

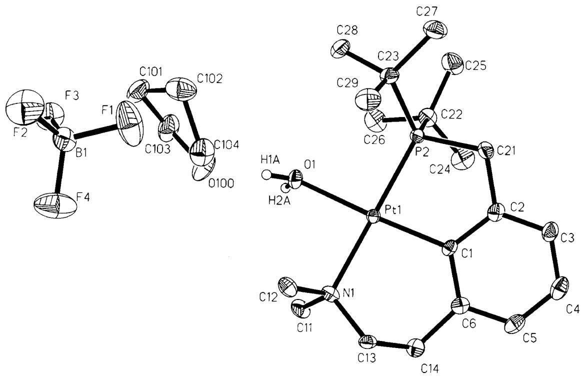

Figure 4. ORTEP view of a molecule of complex **10**.

---

(13) (a) Fulton, J. R.; Holland, A. W.; Fox, D. J.; Bergman, R. G. *Acc. Chem. Res.* **2002**, 35, 44. (b) Bryndza, H. E.; Tam, W. *Chem. Rev.* **1988**, *88*, 1163.

(14) Lukehart, C. M. *Fundamental Transition Metal Organometallic Chemistry*; Wadsworth Inc.: California, 1985.

(15) Recent examples of Pt(II)(OH_2) complexes: (a) van den Broeke, J.; Heeringa, J. J. H.; Chuchuryukin, A. V.; Kooijman, H.; Mills, A. M.; Spek, A. L.; van Lenthe, J. H.; Ruttink, P. J. A.; Deelman, B.-J.; van Koten, G. *Organometallics* **2004**, 23, 2287. (b) Bera, P. S.; Sengupta, P. S.; De, G. S. *Inorg. Reac. Mech.* **2003**, *5*, 65. (c) Sun, X. J.; Jin, C.; Mei, Y. H.; Yang, G. S.; Guo, Z. J.; Zhu, L. G. *Inorg. Chem.* **2004**, *43*, 290. (d) Bera, P. S.; Chandra, S. K.; De, G. S. *Int. J. Chem. Kinet.* **2003**, *53*, 252. (e) Gerdes, G.; Chen, P. *Organometallics* **2003**, *22*, 2217. (f) Anandhi, U.; Holbert, T.; Lueng, D.; Sharp, P. R. *Inorg. Chem.* **2003**, *42*, 1282

(16) Structurally characterized terminal-hydroxo platinum complexes: (a) Flint, B.; Li, J. J.; Sharp, P. R. *Organometallics* **2002**, 21, 997. (b) Straub, B. F.; Rominger, F.; Hoffman, P. *Inorg. Chem. Comm.* **2000**, *3*, 214. (c) Klein, A.; Klinkhammer, K.-W.; Scheiring, T. *J. Organomet. Chem.* **1999**, *592*, 128. (d) Navaro, J. A. R.; Romero, M. A.; Salas, J. M.; Quiros, M. *Inorg. Chem.* **1997**, *36*, 3277. (e) Miyamoto, T. K. *Chem. Lett.* **1994**, 1971. (f) Britten, J. F.; Lippert, B.; Lock, C. J. L.; Pilon, P. *Inorg. Chem.* **1982**, *21*, 1936.

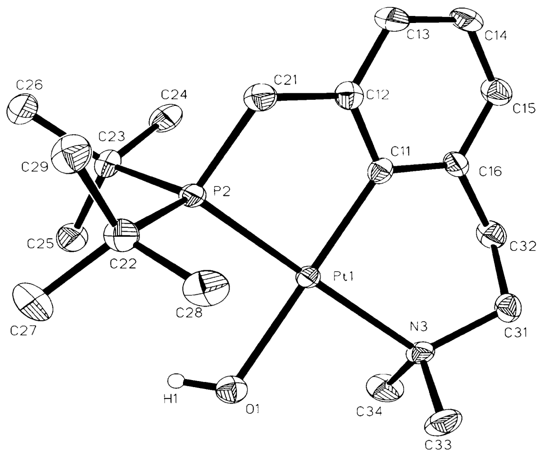

Figure 5. ORTEP view of a molecule of complex **11**.

Table 5. Selected Bond Lengths and Angles of Complex 11

bond length	Å	angle	deg
Pt(1)−C(1)	2.02(5)	C(11)−Pt(1)−N(3)	95.6(16)
Pt(1)−N(3)	2.17(4)	C(11)−Pt(1)−O(1)	177.8(15)
Pt(1)−O(1)	2.09(3)	N(3)−Pt(1)−O(1)	83.6(14)
Pt(1)−P(2)	2.21(13)	C(11)−Pt(1)−P(2)	83.7(13)
O(1)−H(1)	0.82	N(3)−Pt(1)−P(2)	175.6(10)
P(2)−C(21)	1.82(5)	O(1)−Pt(1)−P(2)	97.3(10)
N(3)−C(33)	1.49(6)	Pt(1)−O(1)−H(1)	109.5
C(15)−C(16)	1.34(7)	C(21)−P(2)−Pt(1)	103.4(16)

hydrogen bonds between coordinated H_2O and outer-sphere BF_4. It was shown by van Koten and co-workers that these coordinated water−counteranion interactions have important contribution to the stability of monomeric monocationic aqua complexes.[15a] Additional bond lengths and angles of complex **10** are given in Table 4.

Due to coordination to the metal center, the water molecule becomes more acidic. While no deprotonation was observed by the internal amine base, treatment of **10** with 1 equiv of $(Me_3Si)_2N^-K^+$ resulted in formation of the neutral hydroxo complex **11**. The deprotonation reaction of **10** is reversible, and treatment of **11** with HBF_4 or CF_3SO_3H regenerated the starting aqua complex (Scheme 5).

The $^{31}P\{^1H\}$ NMR spectrum of **11** shows a singlet at 65.15 ppm (J_{Pt-P} = 4185 Hz). The signal due to the hydroxyl ligand appears in the ^1H NMR spectrum at −1.15 ppm as a broad singlet.

Complex **11** was crystallized from a benzene/pentane mixture to give orange-brown prisms suitable for a single-crystal X-ray analysis (Figure 5), which shows the expected square-planar structure. The Pt−O bond length of 2.09(3) Å falls within the range (2.02−2.19 Å) of the few other structurally characterized terminal hydroxo Pt(II) complexes.[16] Other selected bond lengths and bond angles of **11** are given in Table 5.

Scheme 6

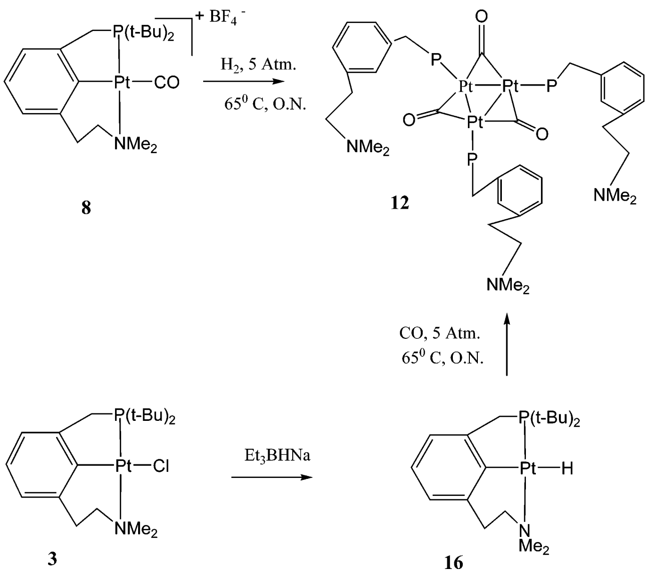

Scheme 7

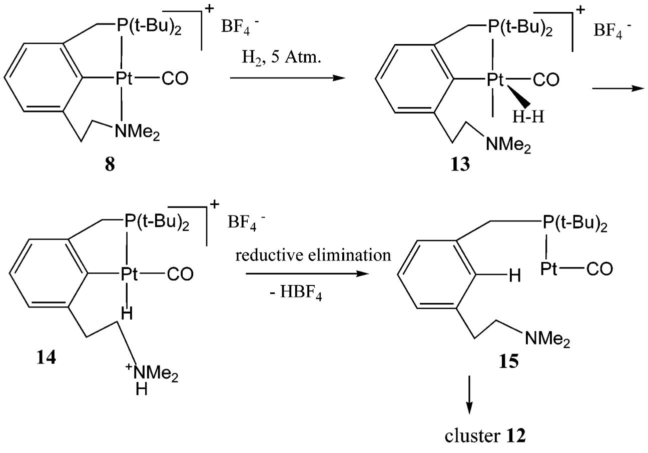

Formation of a Trimeric Cluster. When an acetone solution of **8** was reacted with 5 atm of H_2 gas in a Fischer Porter tube at 65 °C, the novel complex **12** was quantitatively formed after 12 h (Scheme 6). This complex exhibits one resonance at 79.49 ppm in the $^{31}P\{^1H\}$ NMR spectrum with *three sets of Pt satellites* (J_{Pt1-P} = 4742 Hz, J_{Pt2-P} = 460 Hz, J_{Pt3-P} = 357 Hz). Such an unusual NMR pattern led us to consider the possibility of cluster formation, where each phosphorus atom is coupled to three different Pt atoms. In the ^1H NMR spectrum, four aromatic protons were found, while a new proton appears as a singlet at 6.55 ppm. In addition, in the $^{13}C\{^1H\}$ NMR spectrum the ipso carbon was not detected, and in a C−H correlation spectrum an additional C−H cross-peak in the aromatic area was found. The NMR data indicate demetalation of the aromatic ring during the reaction (Scheme 7). To verify this suggestion, we performed the same experiment with D_2 gas. As expected, the signal of the additional aromatic proton at 6.55 ppm disappeared in the ^1H NMR spectrum, while in the ^2H NMR spectrum in CH_2Cl_2 a signal of an aromatic proton at 6.35 ppm was observed. In addition, the signal due to $N(CH_3)_2$ appeared at 1.78 ppm as a singlet without Pt satellites in the ^1H NMR spectrum and at 44.39 ppm in the $^{13}C\{^1H\}$ NMR spectrum. The fact that the two methyl groups of the $N(CH_3)_2$ unit have the same chemical shifts and the platinum satellites are not observed indicates that the amine arm is not coordinated to the metal center and that there is free rotation. Finally, a signal compatible with bridging CO was found at 247.29 ppm (J_{Pt-C} = 724 Hz) in the $^{13}C\{^1H\}$ NMR spectrum and in the IR a μ-CO stretch appeared at 1759 cm^{-1}. Thus, on the basis of NMR data we predicted an approximate configuration of the cluster, while the exact structure was obtained by an X-ray diffraction study. Complex **12** was crystal-

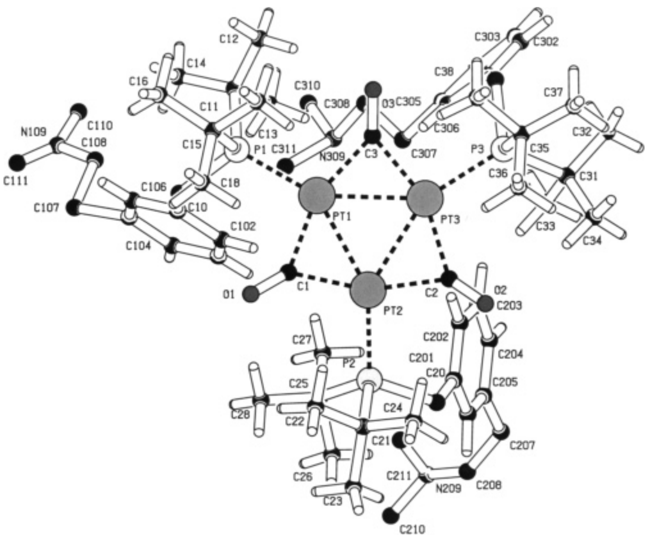

Figure 6. Complex **12**.

Table 6. Selected Bond Lengths and Angles of Complex 12

bond length	Å	angle	deg
Pt(1)−C(3)	2.03(17)	C(3)−Pt(1)-C(1)	154.0(7)
Pt(1)−P(1)	2.29(4)	C(3)−Pt(1)-P(1)	102.9(5)
Pt(1)−Pt(2)	2.67(12)	Pt(1)−Pt(2)-Pt(3)	60.05(4)
Pt(2)−P(2)	2.30(4)	O(1)−C(1)-Pt(1)	138.9(13)
C(1)−O(1)	1.16(19)	0(2)-C(2)−Pt(3)	141.8(14)
P(3)−C(30)	1.86(18)	Pt(1)−Pt(3)-Pt(2)	59.9(3)
Pt(2)−Pt(3)	2.67(12)	P(2)−Pt(2)-Pt(3)	146.3(11)
C(11)−C(14)	1.52(3)	C(1)−Pt(2)-Pt(3)	107.5(5)

lized by slow evaporation of a CH_2Cl_2 solution to give red crystals, the X-ray structure of which (Figure 6) confirmed our spectroscopic structural prediction. Three Pt atoms are connected by metal−metal bonds and by three bridging carbonyl ligands, forming a rigid cluster. The aromatic rings of the ligands underwent demetalation and the amine "arms" were detached from the metal center, the phosphine groups remaining the only coordinated part of the PCN moiety. Selected bond lengths and bond angles of **12** are given in Table 6.

Comparable platinum clusters were obtained by Wong as part of an investigation of the reactivity of *trans*-PtH_2L_2 complexes ($L = PR_3$) with carbon monoxide. These dihydrido complexes react to give different cluster compounds as a result of reductive elimination reactions.[17] Significantly, reaction of the (PCN)PtH complex **16** (which was formed by reaction of **3** with Et_3BHNa at room temperature) with 5 atm of CO under identical conditions resulted in the same complex **12** (Scheme 6).

A plausible mechanism for the cluster-forming reaction is presented in Scheme 7. Coordination of dihydrogen may lead to the five-coordinated intermediate **13** in which the dihydrogen ligand protons become acidic and undergo deprotonation by the internal amine base. Deprotonation of a strong C−H bond by an intramolecular amine base as a result of its coordination to a cationic Rh atom was recently reported.[3b] The opening of the electron-donating amine-"arm" decreases the electron density on the metal center and promotes C−H reductive elimination of the aromatic ring. The resulting coordinatively unsaturated intermediate **15** undergoes trimerization to form the cluster **12**.

In striking difference to the reactivity of complex **8**, the "normal arm" PCN-based carbonyl complex **9** did not react with dihydrogen under the same conditions and remained unchanged (Scheme 6). This result vividly reflects the influence of the amine "arm" length on its hemilability and, as a consequence, on the accessible reactivity patterns.

Summary

The reactivity of complexes based on mixed phosphino-amine (PCN) ligands with different amine "arm" lengths was studied. The new "long arm" PCN-based Pt(II) unsaturated cationic complex (**5**) exhibits interesting reactivity, including coordination of a water molecule to generate an aqua complex (**10**), which was deprotonated to yield a rare monomeric hydroxy complex (**11**). Treatment of the cationic complex (**5**) with carbon monoxide resulted in a stable carbonyl complex (**8**), which reacted with H_2 to form a trimeric cluster (**12**). Parallel investigation of the reactivity of the "normal arm"' PCN-based complexes showed that the longer amine "arm" provides additional reactivity possibilities, since, as expected, it enhances the hemilability effect of the amine ligand. We are currently exploring the effect of this reversible coordination on the activation of various strong bonds and catalysis.

Experimental Section

General Procedures. All experiments with metal complexes and phosphine ligands were carried out under an atmosphere of purified nitrogen in a Vacuum Atmospheres glovebox equipped with an MO 40-2 inert gas purifier or using standard Schlenk techniques. All solvents were reagent grade or better. All nondeuterated solvents were refluxed over sodium/benzophenone ketyl and distilled under an argon atmosphere. Deuterated solvents were used as received. All the solvents were degassed with argon and kept in the glovebox over 4 Å molecular sieves. Commercially available reagents were used as received. The precursor $Pt(COD)(CH_3)Cl$ was prepared according to a literature procedure.[18] ^1H, ^{13}C, and ^{31}P, ^{19}F, and ^2H NMR spectra were recorded at 400, 100, 162, 376, and 61 MHz, respectively, using a Bruker AMX-400 NMR spectrometer and 250 (^1H), 101 (^{31}P), and 235 (^{19}F) using Bruker DPX 250 spectrometer. All spectra were recorded at 23 °C. ^1H NMR and $^{13}C\{^1H\}$ NMR chemical shifts are reported in parts per million downfield from tetramethylsilane. ^1H NMR chemical shifts were referenced to the residual hydrogen signal of the deuterated solvents (7.15 ppm, benzene; 7.24 ppm, chloroform; 5.32 ppm, dichloromethane; 3.58 ppm, tetrahydrofuran). In $^{13}C\{^1H\}$ NMR measurements the signals of C_6D_6 (128.0 ppm), $CDCl_3$ (77.0 ppm), CD_2Cl_2 (53.8 ppm), and d_8-THF (67.5 ppm.) were used as a reference. ^{31}P NMR chemical shifts are reported in ppm downfield from H_3PO_4 and referenced to an external 85% solution of phosphoric acid in D_2O. ^{19}F NMR chemical shifts were referenced to C_6F_6 (−163 ppm), and ^2H NMR chemical shifts were referenced to CD_2Cl_2 (3.58 ppm). Screw-cap 5 mm NMR tubes were used in the NMR follow-up experiments. Abbreviations used in the description of NMR data are as follows: b, broad; s, singlet; d, doublet; t, triplet; q, quartet; m, multiplet.

Preparation of the PCN Ligand 2. 3-(Bromomethyl)-benzyl alcohol, which served as the starting material for the preparation of ligand **2**, was obtained by esterification, bromination, and reduction of 3-(methyl)benzoic acid according to a literature procedure.[12]

---

(17) Clark, H. C.; Goel, A. B.; Wong, C. S. *Inorg. Chim. Acta* **1979**, *159*, 34.

(18) Clark. H. C.; Manzer, L. E. *J. Organomet. Chem.* **1973**, *59*, 411.

(a) Preparation of 3-(Diethylaminomethyl)benzyl Alcohol. In an oven-heated, argon-flushed 100 mL Schlenk flask, equipped with a dropping funnel and a magnetic stirring bar, was dissolved 5.2 mL (0.0050 mol) of degassed Et_2NH in 10 mL of dry THF, and the reaction mixture was cooled to 0 °C. A solution of 3-(bromomethyl)benzyl alcohol (4.6 g, 0.023 mol) in 8 mL of dry THF was added dropwise during 30 min and stirred for a further 24 h. TLC analysis of the solution showed complete conversion to a product. The solvents were removed under vacuum, the residue was treated with 100 mL of diethyl ether, and the organic phase was washed with 10% aqueous KOH solution (2 × 20 mL), dried with Na_2SO_4, filtered, and concentrated in a vacuum. The crude yield was 96%. Distillation (110−120 °C at 0.4 mmHg) resulted in the clean 3-(diethylaminomethyl)benzyl alcohol in 55% yield.

^{1}H NMR ($CDCl_3$): 7.35−7.22 (4H, Ar), 4.63(s, 2H, C$\mathbf{H_2}$−OH), 3.57 (s, 2H, C$\mathbf{H_2}$−N), 3.14 (bs, 1H, CH_2−O**H**), 2.53 (q, 4H, N−(C$\mathbf{H_2}$−CH_3)$_2$), 1.06 (t, 6H, N−(CH_2−C$\mathbf{H_3}$)$_2$). ^{13}C{^{1}H} NMR ($CDCl_3$): 141.10 (s, Ar), 139.33 (s, Ar), 128.25 (s, Ar), 128.22 (s, Ar), 127.65(s, Ar), 125.52 (s, Ar), 64.89 (s, **C**H_2−OH), 57.25 (s, **C**H_2−N), 46.45 (s, N−(CH_2−CH_3)$_2$), 11.22 (s, N−(CH_2−**C**H_3)$_2$) (assignment of ^{13}C{^{1}H} NMR was confirmed by ^{13}C DEPT).

(b) Preparation of 3-(Diethylaminomethyl)benzyl Bromide·HBr Salt. In a 250 mL flask under argon was dissolved 5.48 g (0.028 mol) of 3-(diethylaminemethyl)benzyl alcohol in 55 mL of 48% HBr aqueous solution. The mixture was stirred overnight, and the resulting slightly brown solution was evaporated to dryness under high vacuum. The resulting sticky solid was washed with a copious amount of diethyl ether and stirred overnight, whereupon it became a slightly brown granular solid, which was filtered, washed with diethyl ether, and dried under high vacuum, resulting in 9.14 g (97.2%) of product.

^{1}H NMR (CD_3OD): 7.53−7.37 (4H, Ar), 4.54(s, 2H, C$\mathbf{H_2}$−Br), 4.27 (s, 2H, C$\mathbf{H_2}$−N), 3.14 (q, 4H, N−(C$\mathbf{H_2}$−CH_3)$_2$), 1.22 (t, 6H, N−(CH_2−C$\mathbf{H_3}$)$_2$).

(c) Preparation of Ligand 2. In a 100 mL vessel in the glovebox was dissolved 5.04 g (0.015 mol) of 3-(diethylaminomethyl)benzyl bromide·HBr salt in 45 mL of pure MeOH. A solution of 4.82 g (0.033 mol) of di-*tert*-butyl phosphine in 15 mL of pure MeOH was added, resulting in a colorless solution. The vessel was closed tightly, taken outside the glovebox, and heated with stirring for 48 h under argon. The mixture was cooled to room temperature and reintroduced into the glovebox. Then 9 mL of triethylamine was added, followed by stirring for 30 min. The organic solvent was removed under vacuum, giving a mixture of a white solid and a viscous oil. The residue was treated with a copious amount of diethyl ether, filtered, and dried under vacuum. The resulting snow-white crystals were analyzed by NMR showing some impurities. The product was distilled (bp 140 °C at 0.1 mmHg), yielding 3.85 g (81%) of pure ligand **2**.

^{31}P{^{1}H} NMR (C_6D_6): 35.66 (s). ^{1}H NMR (C_6D_6): 7.55 (s, 1H, Ar), 7.30 (d, J_{H-H} = 7 Hz, 1H, Ar), 7.18 (d, J_{H-H} = 7 Hz, 1H, Ar), 7.12 (d, J_{H-H} = 7 Hz, 1H, Ar), 3.44 (s, 2H, Ar−C$\mathbf{H_2}$−N), 2.74 (d, J_{P-H} = 3 Hz, 2H, Ar−C$\mathbf{H_2}$−P), 2.39 (q, J_{H-H} = 7 Hz, 4H, N−(C$\mathbf{H_2}$−CH_3)$_2$), 1.02 (d, J_{P-H} = 11 Hz, 18H, P(**t-Bu**)$_2$), 0.92 (t, J_{H-H} = 7 Hz, 6H, N−(CH_2−C$\mathbf{H_3}$)$_2$). ^{13}C{^{1}H} NMR ($CDCl_3$): 141.82 (d, J_{P-C} = 12 Hz, Ar), 140.72 (s, Ar), 130.41 (s, Ar), 130.33 (s, Ar), 128.46 (d, J_{P-C} = 8 Hz, Ar), 126.15 (d, J_{P-C} = 2 Hz, Ar). 58.30 (s, Ar−**C**H_2−N), 47.06 (s, N−(**C**H_2−CH_3)$_2$), 31.77 (d, J_{P-C} = 25 Hz, Ar-CH_2−P), 29.87 (d, J_{P-C} = 13 Hz, P(C(**C**H_3)$_3$)$_2$), 29.15 (d, J_{P-C} = 26 Hz, P(**C**(CH_3)$_3$)$_2$), 12.25 (s, N−(CH_2−CH_3)$_2$).

Reaction of the PCN Ligand 2 with (COD)Pt(Cl)Me. Formation of (PCN)PtCl (4). To a THF solution (4 mL) of (COD)Pt(Cl)CH_3 (COD = cyclooctadiene; 104 mg, 0.294 mmol) was added 95 mg (0.294 mmol) of ligand **2** in THF (4 mL). The mixture was stirred at 100 °C for 30 min, resulting in a colorless solution. The ^{31}P{^{1}H} NMR spectrum revealed formation of **4**. The solvent was evaporated, and the complex was washed with pentane and dissolved in benzene. Benzene evaporation yielded 145 mg (0.264 mmol, yield 90%) of **4**. X-ray quality colorless crystals were obtained from a benzene/pentane two-phase mixture at room temperature.

^{31}P{^{1}H} NMR (C_6D_6): 64.31 (s, J_{P-Pt} = 4294 Hz). ^{1}H NMR (C_6D_6): 7.05 (t, J_{H-H} = 8 Hz, 1H, Ar), 6.93 (d, J_{H-H} = 8 Hz, 1H, Ar), 6.71(d, J_{H-H} = 8 Hz, 1H, Ar), 3.59 (s, J_{Pt-H} = 22 Hz, 2H, Ar−C$\mathbf{H_2}$−N), 3.44 (m, 2H, N−C$\mathbf{H_2}$−CH_3), 2.76 (d, J_{P-H} = 11 Hz, J_{Pt-H} = 40 Hz, 2H, Ar−C$\mathbf{H_2}$−P), 2.41 (m, 2H, N−C$\mathbf{H_2}$−CH_3), 1.31 (s, J_{Pt-H} = 15 Hz, 6H, N−CH_2−C$\mathbf{H_3}$), 1.29 (d, J_{P-H} = 14 Hz, 18 H, P−**t-Bu**). ^{13}C{^{1}H} NMR (C_6D_6): 149.22 (d, J_{P-C} = 29 Hz, ipso), 148.91 (d, J_{P-C} = 10 Hz, J_{Pt-C} = 31 Hz, Ar), 146.30 (d, J_{P-C} = 10 Hz, Ar), 123.62 (s, Ar), 121.71 (d, J_{P-C} = 17 Hz, J_{Pt-C} = 80 Hz, Ar), 118.85 (s, J_{Pt-C} = 30 Hz, Ar), 67.15 (d, J_{Pt-C} = 59 Hz, J_{P-C} = 3 Hz, Ar−**C**H_2−P), 56.20 (s, N−**C**H_2−CH_3), 56.18 (s, N−CH_2−**C**H_3), 35.15 (d, J_{P-C} = 61 Hz, P−**C**−(CH_3)$_3$), 35.11 (s, Ar−**C**H_2−N), 29.14 (d, J_{P-C} = 4 Hz, J_{Pt-C} = 22 Hz, P−C−(**C**H_3)$_3$), 12.86 (s, J_{Pt-C} = 23 Hz, N−CH_2−CH_3). ES-MS: m/z^+ 573.55 [calc 574.02] (M + Na^+), 515.62 [calc 515.58] (M − Cl).

Synthesis of [(PCN)Pt]$^+$BF$_4^-$ (5). To a CH_2Cl_2 solution (1 mL) of (PCN)PtCl **3** (20 mg, 0.037 mmol) was added 7 mg (0.037 mmol) of $AgBF_4$, resulting in immediate formation of a white precipitate. After stirring the reaction mixture at room temperature for 1 h, the ^{31}P {^{1}H} NMR spectrum revealed formation of a new complex. The suspension was filtered through Celite, and the solvent was evaporated. The resulting white solid was washed with pentane and benzene and dissolved in THF. After evaporation of THF 24 mg (0.035 mmol, 95% yield) of the white complex **5** was obtained.

Selected NMR data: ^{31}P{^{1}H} NMR (CD_2Cl_2): 69.60 (s, J_{P-Pt} = 3985 Hz). ^{1}H NMR (CD_2Cl_2): 6.96 (d, J_{H-H} = 8 Hz, 1H, Ar), 6.85 (dt, J_{H-H} = 8 Hz, J_{P-H} = 1 Hz, 1H, Ar), 6.62 (d, J_{H-H} = 8 Hz, 1H, Ar), 2.89 (s, 3H, N−C$\mathbf{H_3}$), 2.88 (s, 3H, N−C$\mathbf{H_3}$), 2.84 (m, 2H, CH_2−C$\mathbf{H_2}$−N), 2.72 (m, 2H, C$\mathbf{H_2}$−CH_2−N), 1.35 (d, J_{P-H} = 15 Hz, 18 H, P-**t-Bu**). ^{13}C{^{1}H} NMR (CD_2Cl_2): 150.71 (d, J_{P-C} = 10 Hz, ipso), 142.34 (s, Ar), 125.79 (s, Ar), 125.63 (s, Ar), 122.72 (s, Ar), 122.56 (s, Ar), 64.24 (s, CH_2-**C**H_2−N), 64.23 (s, **C**H_2−CH_2−N), 48.71 (s, N-**C**H_3), 48.70 (s, N-**C**H_3), 34.85 (d, J_{P-C} = 27 Hz, P-**C**-(CH_3)$_3$), 30.61(d, J_{P-C} = 35 Hz, Ar-**C**H_2−P), 28.82 (d, J_{P-C} = 3 Hz, P−C−(**C**H_3)$_3$). ^{19}F NMR (CD_2Cl_2): −162.27 (bs). Anal. Found (Calcd for $C_{22}H_{45}BF_4NOPPt$): C, 40.34 (40.50); H, 7.12 (6.95).

Synthesis of (PCN)Pt(OTf) (6). To a THF (1 mL) solution of (PCN)PtCl **3** (20 mg, 0.037 mmol) was added 10 mg (0.037 mmol) of silver triflate. The mixture was stirred at room temperature for 1 h, resulting in a pink-brown solution. The suspension was filtered through Celite, and the solvent was evaporated. The resulting brown solid was washed with pentane and benzene and dissolved in THF. After evaporation of THF 22 mg (0.033 mmol, 90.2% yield) of (PCN)Pt-OTf **6** was obtained. X-ray quality colorless crystals of complex **6** were obtained from a THF/pentane two-phase mixture at room temperature.

^{31}P{^{1}H} NMR (CD_2Cl_2): 66.52 (s, J_{Pt-P} = 4005 Hz). ^{1}H NMR (CD_2Cl_2): 6.79 (d, J_{HH} = 7 Hz, 1H, Ar), 6.78 (d, J_{HH} = 7 Hz, 1H, Ar), 6.47 (d, J_{HH} = 7 Hz, 1H, Ar), 2.59 (s, J_{PtH} = 20 Hz, 3H, N−C$\mathbf{H_3}$), 2.58 (s, J_{PtH} = 20 Hz, 3H, N−C$\mathbf{H_3}$), 2.55 (d, J_{PH} = 10 Hz, J_{PtH} = 44 Hz, 2H, Ar−C$\mathbf{H_2}$−P), 2.34 (m, 2H, CH_2−C$\mathbf{H_2}$−N), 1.92 (m, 2H, C$\mathbf{H_2}$−CH_2−N), 1.15 (d, J_{PH} = 14 Hz, 18 H, P−**t-Bu**). ^{13}C{^{1}H } NMR (CD_2Cl_2): 150.33 (d, J_{PH} = 10 Hz, ipso), 142.72 (s, Ar), 125.30 (s, Ar), 125.24 (s, Ar), 122.07 (s, Ar), 122.91 (s, Ar), 64.14 (s, Ar−CH_2−**C**H_2−N), 64.12 (s, Ar−**C**H_2−CH_2−N), 49.18 (s, N−**C**H_3), 49.17 (s, N−**C**H_3), 34.42 (d, J_{PC} = 36 Hz, P−**C**−(CH_3)$_3$), 32.55 (d, J_{PC} = 26 Hz, Ar−**C**H_2−P), 35.32 (s, Pt−O−SO_2−**C**F_3), 28.89 (d, J_{PC} = 3 Hz, P−C−(**C**H_3)$_3$), ^{19}F NMR (CD_2Cl_2): −77.61 (s). ES-MS: m/z^+ 501.32 [calc 501.59] (M − OTf), m/z^- 148.82 [calc 149.07] (OTf $^-$).

Synthesis of [(PCN)Pt]$^+$BF$_4^-$ (7). To a CH_2Cl_2 solution (1 mL) of (PCN)PtCl **4** (20 mg. 0.036 mmol) was added 7 mg

(0.036 mmol) of $AgBF_4$, resulting in immediate formation of a yellow precipitate. After stirring the reaction mixture at room temperature for 1 h, the $^{31}P\{^1H\}$ NMR spectrum revealed formation of a new complex. The suspension was filtered through Celite, and the solvent was evaporated. The resulting yellow solid was washed with pentane and benzene and dissolved in THF. After evaporation of THF 21 mg (0.035 mmol, 96% yield) of complex **7** was obtained.

$^{31}P\{^1H\}$ NMR (C_6D_6): 63.91 (s, J_{PPt} = 4195 Hz). ^1H NMR (C_6D_6): 6.88 (t, J_{HH} = 7 Hz, 1H, Ar), 6.67 (d, J_{HH} = 7 Hz, 1H, Ar), 6.42 (d, J_{HH} = 7 Hz, 1H, Ar), 3.38 (m, 2H, N−C**H₂**−CH_3), 3.34 (s, J_{PtH} = 24 Hz, 2H, Ar−C**H₂**−N), 2.57 (m, 2H, N−C**H₂**−CH_3), 2.47 (d, J_{PH} = 9 Hz, 2H, Ar−C**H₂**−P), 1.26 (t, J_{PH} = 7 Hz, 6H, N−CH_2−C**H₃**), 1.15 (d, J_{PH} = 14 Hz, 18H, P−t-Bu). $^{13}C\{^1H\}$ NMR (C_6D_6): 148.41 (d, J_{PC} = 1, ipso), 146.68 (d, J_{PC} = 9 Hz, Ar), 124.83 (s, Ar), 123.57 (s, Ar), 121.78 (d, J_{PC} = 14 Hz, Ar), 119.09 (s, Ar), 67.78 (s, N−**C**H_2−CH_3), 65.30 (s, Ar−**C**H_2−N), 55.70 (s, N−**C**H_2−CH_3), 34.74 (d, J_{PC} = 26 Hz, P−**C**−(CH_3) ₃), 32.84 (d, J_{PC} = 36 Hz, Ar−**C**H_2−P), 28.68 (d, J_{PC} = 4 Hz, P−C−(**C**H_3) ₃), 13.97 (s, N−CH_2−**C**H_3). ^{19}F NMR (CD_2Cl_2): −162.14 (bs). Anal. Found (Calcd for $C_{24}H_{49}BF_4NOPPt$): C, 42.46 (42.36); H, 7.18 (7.26).

Synthesis of (PCN)Pt(CO) Complex (8). To a CH_2Cl_2 solution (0.7 mL) of $[(PCN)Pt]^+BF_4^-$ (**5**) (20 mg, 0.034 mmol) in a screw up NMR tube was injected 2.4 mL (0.080 mmol) of CO gas. The $^{31}P\{^1H\}$ NMR spectrum revealed the immediate formation of (PCN)PtCO complex **8**. The solvent was evaporated, and the resulting white solid was washed with pentane, benzene, and THF and dissolved in CH_2Cl_2. The solvent was evaporated, yielding 19 mg (0.032 mmol, 88.2% yield) of **8** as white crystals. X-ray quality pale yellow crystals of **8** were obtained by slow evaporation of a CH_2Cl_2 solution at room temperature.

$^{31}P\{^1H\}$ NMR ($CDCl_3$): 81.04 ppm (s, J_{PtP} = 3045 Hz). ^1H NMR ($CDCl_3$): 7.16 (d, J_{HH} = 7 Hz, 1H, Ar), 6.98 (dt, J_{HH} =7 Hz, J_{PH} = 2 Hz, 1H, Ar), 6.85 (d, J_{HH} = 7 Hz, 1H, Ar), 3.39 (d, J_{PH} = 7 Hz, J_{PtH} = 44 Hz, 2H, Ar−C**H₂**−P), 3.19 (s, J_{PtH} = 28 Hz, 3H, N−C**H₃**), 3.19 (s, J_{PtH} = 18 Hz, 3H, N−C**H₃**), 2.93 (m, 2H, CH_2−C**H₂**−N), 2.76 (m, 2H, C**H₂**−CH_2−N), 1.27 (d, J_{PH} = 15 Hz, 18 H, P−**t-Bu**). $^{13}C\{^1H\}$ NMR ($CDCl_3$): 181.14 (d, J_{PC} = 8 Hz, $J_{Pt\ C}$ = 981 Hz, Pt−**C**O), 150.65 (d, J_{PC} = 9 Hz, ipso), 142.41 (d, J_{PC} = 1 Hz, Ar), 128.77 (s, Ar), 126.53 (s, Ar), 122.64 (s, Ar), 122.46 (s, Ar), 63.09 (s, Ar−CH_2−**C**H_2−N), 63.07 (s, Ar−**C**H_2−CH_2−N), 55.12 (s, N−**C**H_3), 55.10 (s, N−**C**H_3), 36.19 (d, J_{PC} = 22 Hz, P−**C**−$(CH_3)_3$), 33.82 (d, J_{PC} = 23 Hz, Ar−**C**H_2−P), 29.01 (d, J_{PC} = 3 Hz, P−C−(**C**H_3)₃). ^{19}F NMR ($CDCl_3$): −153.01 (s). IR (film): (Pt−**CO**) 2082 cm^{-1}. ES-MS: *m/z*$^+$ 501.57 [calc 501.59] (M − CO), *m/z*$^-$ 87.05 [calc 86.80] (BF_4^-).

Synthesis of (PCN)Pt(CO) (9). To a CH_2Cl_2 solution (0.7 mL) of $[(PCN)Pt]^+BF_4^-$ **7** (20 mg, 0.033 mmol) in a screw up NMR tube was injected 2.4 mL (0.08 mmol) of CO gas. The $^{31}P\{^1H\}$ NMR spectrum revealed the immediate formation of a new complex. After evaporation, the resulting white solid was washed with pentane, benzene, and THF and dissolved in dichloromethane, which was evaporated to yield 19 mg (0.0 29 mmol) of **9** as white crystals in 87.2% yield.

$^{31}P\{^1H\}$ NMR ($CDCl_3$): 80.16 (s, J_{P-Pt} = 3264 Hz). ^1H NMR ($CDCl_3$): 7.19 (d, J_{H-H} = 7 Hz, 1H, Ar), 7.15 (t, J_{H-H} = 7 Hz, 1H, Ar), 7.11 (d, J_{H-H} = 7 Hz, 1H, Ar), 4.52 (s, J_{Pt-H} =16 Hz, 2H, Ar−C**H₂**−N), 3.67 (d, J_{P-H} = 15 Hz, 2H, Ar−C**H₂**−P), 3.65 (m, 2H, N−C**H₂**−CH_3), 3.58 (m, 2H, N−C**H₂**−CH_3), 1.48 (t, J_{H-H} = 14 Hz, 6H, N−CH_2−C**H₃**), 1.40 (d, J_{P-H} = 15 Hz, 18 H, P−**t-Bu**). $^{13}C\{^1H\}$ NMR ($CDCl_3$): 185.19 (d, J_{P-C} = 6 Hz, Pt−CO), 160.56 (d, J_{P-C} = 1 Hz, ipso), 153.82 (s, Ar), 148.98 (d, J_{P-C} = 8 Hz, Ar), 129.61 (s, Ar), 123.10 (d, J_{P-C} = 18 Hz, Ar), 121.16 (s, J_{Pt-C} = 16 Hz, Ar), 70.76 (d, J_{P-C} = 2 Hz, J_{Pt-C} = 37.5 Hz, Ar−**C**H_2−N), 69.78 (s, N−**C**H_2−CH_3), 60.64 (s, N−**C**H_2−CH_3), 37.3 (d, J_{P-C} = 37 Hz, Ar−**C**H_2−P), 38.35 (d, J_{P-C} = 26 Hz, P−**C**−(CH_3) ₃), 30.73 (d, J_{P-C} = 3 Hz, P−C−(**C**H_3)₃), 15.16 (s, J_{Pt-C} = 23 Hz, N−CH_2−**C**H_3). ^{19}F NMR

Table 7. Experimental Crystallographic Data for Complexes 4, 6, 8, 10, 11, and 12

empirical formula	C20H31ClPNPt,	C20H33O3PNF3SPt	C20H33OPNPt + BF4	C19H45OPNPt + BF4 + C4H8O	C19H28OPNPt + BF4 + C4H8O	C121·5H132 Cl3N6010P6Pt6
fw	546.97	650.59	616.34	678.45	512.48	3299.04
radiation	Mo Kα (0.710)	Mo Kα (0.710)	Mo Kα (0.710)	Mo Kα (0.710)	Mo Kα (0.710)	Mo Kα (0.710)
cryst syst	monoclinic	orthorhombic	monoclinic	monoclinic	monoclinic	triclinic
space group	$P2(1)/n$ (No.14)	$P2(1)2(1)2(1)$ (No.19)	$P2_1/c$ (No.14)	$P2_1/c$ (No.14)	$P2_1/c$ (No.14)	$P\bar{1}$ (No.2)
unit cell						
a/Å	12.065(2)	7.459(1)	8.5540(17)	9.6500(1)	20.075(4)	13.147(3)
b/Å	13.391(3)	16.565(2)	15.064(3)	14.9410(2)	7.978(2)	22.554(5)
c/Å	13.625(3)	18.674(2)	17.654(4)	18.9480(3)	12.800(3)	26.983(5)
α/deg						104.11(3)
β/deg	104.69(3)		93.03(3)	97.124(1)		93.39(3)
γ/deg						94.08(3)
D_c/Mg/m^3	1.706	1.873	1.802	1.678	1.713	1.420
μ(Mo Kα)/mm^{-1}	6.792	6.287	7.291	5.332	7.147	5.579
cryst size/mm^3	0.2 × 0.1 × 0.1	0.3 × 0.1 × 0.1	0.05 × 0.05 × 0.05	0.2 × 0.1 × 0.1	0.1 × 0.05 × 0.05	0.2 × 0.2 × 0.1
total/unique no. of rflns	9045, 4792	41 158, 3125	35 510, 6337	42 343, 4847	25 084, 6133	66 469, 15 823
R_{int}	0.07	0.086	0.086	0.087	0.062	0.064
no. of params, restraints	225,0	279, 0	270, 0	309, 0	210, 0	1320, 31
R1, wR2	0.036,0.047	0.0283, 0.0317	0.036, 0.058	0.0327, 0.0456	0.0293, 0.0421	0.064, 0.18
resid density/e Å^3	1.326	1.46	1.87	1.64	1.322	3.107

(CDCl$_3$): −154.29 (s). IR (film): 2085 cm^{-1} (Pt−**C**O). ES-MS: m/z^{+} 515.36 [calc 515.58] (M − CO), m/z^{-} 86.87 [calc 86.80] (BF$_4^-$).

Preparation of the Aqua Complex 10. To a CH$_2$Cl$_2$ solution (1 mL) of the cationic complex **5** (20 mg, 0.034 mmol) was added (0.63 μL, 0.034mol) of H$_2$O, and the ^{31}P{^{1}H} NMR spectrum revealed formation of a new complex. The solvent was evaporated, and the resulting white solid was washed with pentane and benzene and dissolved in THF. The THF solvent was evaporated to yield 19.5 mg (0.032 mmol, 94.7% yield) of complex **10**. X-ray quality colorless prismatic crystals of **10** were obtained from a concentrated THF solution, after slow addition of pentane at room temperature.

^{31}P{^{1}H} NMR (CD$_2$Cl$_2$): 67.52 ppm, $J_{\mathrm{Pt-P}}$ = 3950 Hz. ^{1}H NMR (CD$_2$Cl$_2$): 6.88 (t, J_{HH} = 7 Hz, 1H, Ar), 6.78 (d, J_{HH} = 7 Hz, 1H, Ar), 6.50 (d, J_{HH} = 7 Hz, 1H, Ar), 5.12 (bs, 2H, Pt−**OH$_2$**), 2.23 (m, 2H, CH$_2$−C**H$_2$**−N), 1.85 (m, 2H, C**H$_2$**−CH$_2$−N), 1.11 (d, J_{PH} = 14 Hz, 18 H, P−**t-Bu**). ^{13}C{^{1}H } NMR (C$_6$D$_6$): 150.70 (d, J_{PC} = 10 Hz, ipso), 142.81 (s, J_{PtC} = 90 Hz, Ar), 125.43 (s, Ar), 125.35 (s, Ar), 121.70 (s, Ar), 121.54 (s, Ar), 64.01 (s, Ar−CH$_2$−**C**H$_2$−N), 64.03 (s, Ar−**C**H$_2$−CH$_2$−N), 48.78 (s, N−**C**H$_3$), 48.75 (s, N−**C**H$_3$), 34.71 (d, J_{PC} = 26 Hz, P−**C**−(CH$_3$)$_3$), 32.27 (d, J_{PC} = 25 Hz, Ar−**C**H$_2$−P), 28.97 (d, J_{PC} = 2 Hz, P−C−(**C**H$_3$)$_3$). ^{19}F NMR (CD$_2$Cl$_2$): −150.72 (s). Anal. Found (Calcd for C$_{20}$H$_{43}$BF$_4$NOPPt): C, 38.49 (38.35); H, 7.08 (6.92).

Preparation of the (PCN)Pt(OH) (11). To a THF solution (1.5 mL) of the aqua complex **10** (20 mg, 0.033 mmol) was added 7.1 mg (0.033 mmol) of (Me$_3$Si)$_2$NK. Deprotonation of the coordinated water molecule and formation of the neutral hydroxo **11** complex were revealed by the ^{31}P{^{1}H} NMR spectrum. The solvent was evaporated, and the resulting orange solid was washed with pentane and dissolved in benzene. The benzene was evaporated to yield 16 mg (0.031 mmol, 93.6% yield) of complex **11**. Complex **11** was crystallized by careful pentane addition to a concentrated benzene solution, leading after 3 days at room temperature to orange-brown crystals.

^{31}P{^{1}H} NMR (C$_6$D$_6$): 65.15 (s, J_{PPt} = 4185 Hz). ^{1}H NMR (C$_6$D$_6$): 7.03 (dd, $J_{\mathrm{P-H}}$ = 2 Hz, $J_{\mathrm{H-H}}$ = 7 Hz, 1H, Ar), 6.83 (t, $J_{\mathrm{H-H}}$ = 7 Hz, 1H, Ar), 6.74 (d, $J_{\mathrm{H-H}}$ = 7 Hz, 1H, Ar), 2.74 (s, $J_{\mathrm{Pt-H}}$ = 23 Hz, 3H, N−C**H$_3$**), 2.73 (s, $J_{\mathrm{Pt-H}}$ = 22 Hz, 3H, N−C**H$_3$**), 2.55 (m, 2H, CH$_2$−C**H$_2$**−N), 2.23 (m, 2H, C**H$_2$**−CH$_2$−N), 1.20 (d, J_{PH} = 14 Hz, 18 H, P−**t-Bu**), −1.15 (bs, 1H, Pt−O**H**). ^{13}C{^{1}H} NMR (C$_6$D$_6$): 150.61 (d, $J_{\mathrm{P-C}}$ = 10 Hz, ipso), 143.29 (s, Ar), 124.67 (d, J_{PC} = 2 Hz, Ar), 122.66 (s, Ar), 121.50 (s, Ar), 121.34 (s, Ar), 62.84 (s, CH$_2$−**C**H$_2$−N), 62.82 (s, **C**H$_2$−CH$_2$−N), 47.45 (s, N−**C**H$_3$), 47.43 (s, N−**C**H$_3$), 34.77 (d, J_{PC} = 35 Hz, Ar−**C**H$_2$−P), 33.82 (d, $J_{\mathrm{P-C}}$ = 27 Hz, P−**C**−(CH$_3$)$_3$), 29.09 (d, $J_{\mathrm{P-C}}$ = 3 Hz, $J_{\mathrm{Pt-C}}$ = 20 Hz, P−C−(**C**H$_3$)$_3$). Anal. Found (Calcd for C$_{13}$H$_{22}$NOPPt): C, 36.15 (36.95); H, 5.04 (5.11).

Synthesis of the Trimeric Cluster 12. An acetone solution (3 mL) of complex **8** (20 mg, 0.32 mmol) in a Fischer Porter tube was charged with 5 atm of H$_2$. The solution was stirred at 65 °C for 12 h, and an orange-red color appeared. The ^{31}P-{^{1}H} NMR spectrum of the solution revealed formation of a new complex. The solution was evaporated, resulting in a red solid, which was washed with pentane and THF and dissolved in methylene chloride. Evaporation of the solvent resulted in red crystals of complex **12** (12.4 mg, 0.01 mmol of trimeric cluster, 93.7% yield).

^{31}P{^{1}H} NMR (CD$_2$Cl$_2$): 79.49 (s, $J_{\mathrm{Pt1-P}}$ = 4742 Hz, $J_{\mathrm{Pt2-P}}$ = 460 Hz, $J_{\mathrm{Pt3-P}}$ = 357 Hz). ^{1}H NMR (CD$_2$Cl$_2$): 6.55 (s, 1H, Ar), 6.47 (d, J_{HH} = 8 Hz, 1H, Ar), 6.25 (d, J_{HH} = 8 Hz, 1H, Ar), 6.14 (d, J_{HH} = 8 Hz, 1H, Ar), 3.21 (d, J_{PH} = 2 Hz, J_{PtH} = 44 Hz, 2H, Ar−C**H$_2$**−P), 2.21 (m, 2H, CH$_2$−C**H$_2$**−N), 1.90 (m, 2H, C**H$_2$**−CH$_2$−N), 1.78 (s, 6H, N−(C**H$_3$**)$_2$), 0.32 (d, J_{PH} = 13 Hz, 18 H, P−**t-Bu**). ^{13}C{^{1}H } NMR (CD$_2$Cl$_2$): 247.29 (s, J_{PtC} = 724 Hz, μ-**C**O), 137.9 (s, Ar), 135.8 (s, Ar), 131.74 (bs, Ar), 129.71 (bs, Ar), 128.80 (s, Ar), 126.92 (s, Ar), 68.11 (s, Ar−CH$_2$−**C**H$_2$−N), 59.80 (s, Ar−**C**H$_2$−CH$_2$−N), 44.39 (s, N−(**C**H$_3$)$_2$), 38.55 (d, J_{PC} = 10 Hz, P−**C**−(CH$_3$)$_3$), 38.25 (d, J_{PC} = 12 Hz, P−C−(**C**H$_3$)$_3$), 30.13 (bs, Ar−**C**H$_2$−P). IR: (μ-CO) 1759 cm^{-1}. Anal. Found (Calcd for C$_{60}$H$_{124}$N$_3$O$_3$P$_3$Pt$_3$): C, 44.73 (44.65); H, 7.78 (7.74).

X-ray Structure Determination and Refinement of Complexes 4, 6, 8, 10, 11, and 12. The crystals were mounted in a nylon loop and flash frozen in a cold nitrogen stream (120 K) on a Nonius Kappa CCD with Mo Kα radiation (λ = 0.71071 Å). Accurate unit cell dimensions were obtained from 20° of data. The data were processed with the Denzo-Scalepack package. The structure was solved by direct methods (SHELXS-97) and refined by full-matrix least-squares (SHELXL-97). Idealized hydrogen atoms were placed and refined in the riding mode. Crystal data are given in Table 7.

Acknowledgment. This work was supported by the Israel Science Foundation and by the Helen and Martin Kimmel Center for Molecular Design. D.M. is the holder of the Israel Matz Professorial Chair of Organic Chemistry.

Supporting Information Available: Tables giving X-ray crystallographic data for complexes **4**, **6**, **8**, and **10**−**12**. This material is available free of charge via the Internet at http://pubs.acs.org.

OM049182M